AAPS PharmSciTech (2020) 21:170
DOI: 10.1208/s12249-020-01711-2

Check for updates

Research Article

Enhanced Oral Bioavailability of Felodipine from Solid Lipid Nanoparticles Prepared Through Effervescent Dispersion Technique

Yingmeng He,[1] Chenglin Zhan,[1] Chao Pi,[1] Ying Zuo,[2] Siyun Yang,[3] Mei Hu,[1] Yuntian Bai,[4] Ling Zhao,[1,5] and Yumeng Wei[1,5]

Received 11 December 2019; accepted 13 May 2020

Abstract. Felodipine (FLD), a dihydropyridine calcium channel blocker with excellent antihypertensive effect, is poorly soluble and undergoes extensive hepatic metabolism, which lead to poor oral bioavailability (about 15%) and limit its clinic application. The goal of this study was to develop solid lipid nanoparticles (SLNs) loading FLD to improve the oral bioavailability. The FLD loaded solid lipid nanoparticles (FLD-SLNs) were prepared by the effervescent dispersion technique developed by our laboratory, which might have some advantages over traditional methods. The FLD-SLNs showed desired particle characteristics with particle size (198.15 ± 1.82 nm), poly dispersity index (0.26 ± 0.02), zeta-potential (−25.53 ± 0.60 mV), entrapment efficiency (95.65 ± 0.70%), drug loading (2.33 ± 0.10%), and a spherical appearance. Pharmacokinetic results showed that the FLD-SLNs presented 3.17-fold increase in area under the curve ($AUC_{(0\text{-}t)}$) compared with free FLD after oral administration in beagle dogs, which indicated that SLNs prepared using the effervescent dispersion technique can improve the bioavailability of lipophilic drugs like felodipine by enhancement of absorption and reduction first-pass metabolism.

KEY WORDS: effervescent dispersion technique; felodipine; oral bioavailability; solid lipid nanoparticles.

INTRODUCTION

Oral delivery is the most common administration route for medications but faces with challenges from the poor aqueous solubility of drug candidates (1). Improving the oral bioavailability of poorly water-soluble drugs is one of the main goals of drug development in recent decades (2). Therefore, particle size reduction, solubilization, salt formation, and preparation of solid dispersion have been developed to enhance the oral bioavailability by increasing the dissolution (3–6). Albeit achieving a big progress, these techniques are still facing several disadvantages and limitations. The solubilization techniques are mainly applied to liquid preparation, which suffers from poor patient's compliance and stability (6), precipitation in gastrointestinal tract due to pH variation seriously impedes the development of salt formation (6,7), while the size reduction and solid dispersion techniques are limited to BCS II drugs that are poorly soluble with high permeability. It is more challenging for drugs that are poorly soluble with low permeability or with extensive first-pass metabolism.

Inspired by the enhanced oral absorption from high-fat diet, lipid-based nanocarriers (LBN) have gained wide attention and great success in oral drug delivery (8–10). The underlying mechanisms concern the lipid digestion and absorption (11). The secondary nanostructures produced during lipolysis may solubilize the poorly soluble drugs, transport them across the unstirred water layer, and facilitate transepithelial permeation of the drug molecules (12–14). In addition, the lipids may enhance the lymphatic transport, being advantageous to bypass the hepatic metabolism and improve oral bioavailability (15). Solid lipid nanoparticles (SLNs) are colloidal dispersions composed of a solid lipid phase stabilized by surfactants. Being as one typical LBN,

Yingmeng He and Chenglin Zhan contributed equally to this work.

[1] Key Laboratory of Medical Electrophysiology, Ministry of Education, School of Pharmacy, Southwest Medical University, No.319, Sanduan of Zhongshan Rd., Jiangyang District, Luzhou, 646000, Sichuan, People's Republic of China.
[2] The Affiliated Hospital of Traditional Chinese Medicine of Southwest Medical University, No.16, Chunhui Road, Longma Tan District, Luzhou, 646000, Sichuan Province, People's Republic of China.
[3] Department of Pharmacy of Nanchong Central Hospital, No.128, Dabei Street, Shunqing District, Nanchong, 637000, Sichuan Province, People's Republic of China.
[4] Pharmaceutical Science (English) (2015), Shenyang Pharmaceutical University, No.103 Wenhualu Street, Shenhe District, Shenyang, 110000, Liaoning, People's Republic of China.
[5] To whom correspondence should be addressed. (e–mail: zhaoling-998@163.com; weiyumeng-268@163.com)

aaps
Published online: 11 June 2020

SLNs have been successfully applied to enhance the oral bioavailability of poorly water soluble drugs, such as nitrendipine (16), nimodipine (17), and ramipril (18). Besides, SLNs exhibit great potentiality to bypass first-pass metabolism by enhancing lymphatic transportation (19). Although being invented in 1990s, the industrialization of SLNs is severely hindered by the preparation technique, *i.e.*, the high-pressure homogenization (HPH) and solvent emulsification evaporation technique (20). HPH is the most popular technique but suffers from energy consuming, heat-induced drug degradation, super-cooled melt, and a broad size distribution (21,22). The latter is environmentally unfriendly due to the evaporation of organic solvents.

We once developed an effervescent dispersion technique to prepare liposomes (23–25), which combined the solid dispersion and effervescent. The mechanism of this method is shown in Fig. 1. In the process, citric acid is dispersed in a solid lipid film of phospholipids and drugs. Following addition of $NaHCO_3$ aqueous solution, the lipid films are quickly dispersed by the effervescent effects and spontaneously form drug loaded liposomes (23–25). The violent effervescence throughout the whole film provides powerful forces for its dispersion, leading to small and uniform liposomes. Therefore, there is no requirement for the external energy input. Similarly, the effervescent dispersion technique may be applied to the preparation of SLNs. Compared with the current techniques, this technique is rather simple, superior in size control, energy efficient, and absence of thermal stressless.

Felodipine (FLD) is a dihydropyridine calcium channel blocker widely used in the treatment of hypertension with the advantages of selective dilation of small arteries, no obvious inhibition of myocardium, no influence on glomerular filtration rate, and reduction of organ damage (26–28). However, due to its poor solubility (solubility < 0.5 mg/L) and extensive hepatic first-pass metabolism, the oral bioavailability of FLD is very poor of only 15%, and the clinic application is greatly limited (29–32). Therefore, FLD-loaded SLNs (FLD-SLNs) were developed by a modified effervescent dispersion technique in this study to improve the oral bioavailability of FLD. The applicability of the effervescent dispersion technique to the preparation of SLNs was also validated.

MATERIALS AND METHODS

Materials

FLD was purchased from Changzhou Ruiming Pharmaceutical Co., Ltd. (Jiangsu, China). Glyceryl behenate, mannitol, citric acid, and Tween-80 were obtained from Chengdu Jinshan Chemical Reagent Co., Ltd. (Sichuan, China). Poloxamer 188, Hexadecyltrimethylammonium bromide (HTAB) was obtained from Chengdu Best Reagent Co., Ltd. (Sichuan, China). Methanol and acetonitrile (HPLC grade) and other agents were purchased by Chengdu Kelong Chemical Reagent Factory (Sichuan, China).

Animals

Beagle dogs were obtained from Chengdu Dashuo Experimental Animal Co., Ltd. (Sichuan, China, permit number scxk (chuan) 2013–24). The animals were fed at a temperature of 20 ± 2°C, with relative humidity of 50–60% and 12 h light-dark cycles. All the animals were fasted overnight with free access to water before the experiment. Animal studies were approved by the Committee on the Ethics of Animal Experiments of the Southwest Medical University (No 2015DW040).

METHODS

Preparation of FLD-SLNs

FLD-SLNs were produced by the modified effervescent dispersion technique as our previous research described (24,25). In brief, the FLD was mixed with lipid (glyceryl behenate), surfactant (Tween-80, poloxamer 188), and citric acid and dissolved in 2 mL of ethanol**.** The lyophilized protective agent (mannitol) was added into 10 mL of sodium bicarbonate aqueous solution (0.75% $NaHCO_3$, w/v) and stirred for 5 min at 60°C. The main purpose of adding citric acid and sodium bicarbonate was to produce an effervescent effect. Then, the ethanol solution was introduced into the 0.75% $NaHCO_3$ solution under stirring. Following removal of ethanol by evaporation, the temperature of the mixture was quickly decreased to about 4°C and stirred for further 2 h. The resulted suspensions was lyophilized by a freeze dry system (LGJ-18C; Fourth-Ring Science Instrument plant Beijing Co., Ltd., Beijing, China) to obtain a solid freeze-dried product.

Optimization of Formulation with Orthogonal Experimental Design

The effects of the amount of FLD, glyceryl behenate, Tween-80, and mannitol on particle size (PS), polydispersity index (PDI), zeta potential (ZP) and entrapment efficiency (EE) of FLD-SLNs were investigated by single-factor method. The specific prescription composition was shown in Table I.

On the basis of single-factor experiment, an orthogonal experimental design was introduced to optimize the formulation of FLD-SLNs. Four factors of FLD-SLNs formulation, including the amount of glyceryl behenate (A), mannitol (B), FLD (C), and Tween-80 (D), and three levels for each factor were arranged according to a L_9 (3^4) orthogonal experiment table. The EE was selected as the evaluation index, which was as high as possible. The result was analyzed by intuitive analysis and variance analysis methods. SPSS17 software was used for generation and evaluation of the orthogonal experiment design.

Confirmatory Test

In order to verify the reproducibility of the preparation process of FLD-SLNs, three batches of FLD-SLNs samples (N0.1, NO.2, and NO.3) were prepared by the optimized prescription. The PS, PDI, ZP, EE, and DL of the three batches samples were observed.

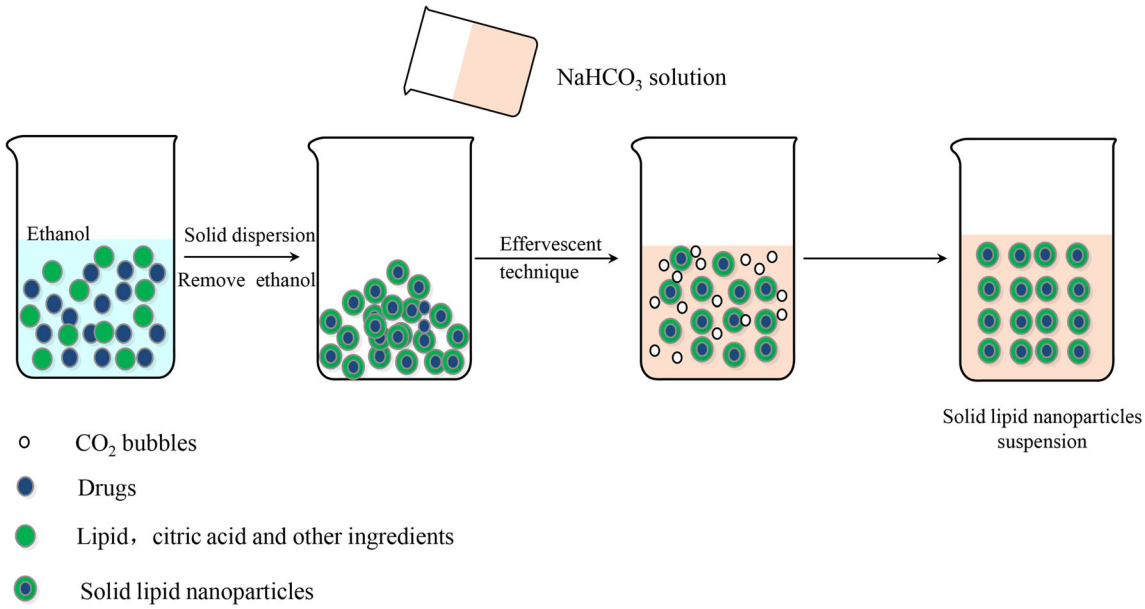

Fig. 1. The mechanism of effervescent dispersion technology

CHARACTERIZATION OF FLD-SLNS

Determination of Particle Size (PS), PDI and Zeta-Potential (ZP)

The PS, PDI, and ZP of FLD-SLNs were determined using NanoBrook 90Plus Zeta (Brookhaven Instruments, USA) after the solid freeze-dried nanoparticles were suspended in ultrapure water (33).

Entrapment Efficiency (EE) and Drug Loading (DL)

The quantification of FLD was carried out by UV-visible spectrophotometer (UV1700-PC; Shanghai Phenix Optical Scientific Instrument Co., Ltd., China) at 361 nm. Good linearity was obtained between 1.000 and 100.000 μg/mL for methanol samples ($A = 0.0164C\text{-}0.0032$, $R = 0.9999$). The EE and DL were calculated by subtracting the amount of free drug from initial amount of drug taken. To separate the free drug, the prepared SLN was centrifuged at 8000 rpm for 10 min at 4°C temperature using cool ultracentrifuge (TGL-20 M super centrifuge; Xiangyi Centrifuge Instrument Co., Ltd., Hunan, China). The 2 mL of supernatant was vortex-mixed with 2 mL of methanol for 10 min, and then the mixture liquid was filtrated through a 0.22 μm hydrophobic millipore membrane to measure the amount of free drug in SLN. The total drug included in SLN was also determined by UV-visible spectrophotometer as

Table I. Prescriptions and results of single-factor test ($n = 3$)

No	Temperature (°C)	Glyceryl behenate (g)	Tween-80 (g)	FLD (g)	Mannitol (g/100 mL)	PS (nm)	PDI	ZP (-mV)	EE (%)
Optimization of glyceryl behenate									
F1	60	0.10	0.60	0.02	5	185.31 ± 3.28	0.27 ± 0.01	26.24 ± 1.87	80.29 ± 0.54
F2	60	0.02	0.60	0.02	5	198.32 ± 0.27	0.32 ± 0.04	24.17 ± 0.31	94.33 ± 0.27
F3	60	0.05	0.60	0.02	5	197.11 ± 2.06	0.28 ± 0.05	25.21 ± 0.26	96.42 ± 0.18
F4	60	0.08	0.60	0.02	5	189.89 ± 0.89	0.27 ± 0.14	25.32 ± 0.23	92.74 ± 0.65
Optimization of FLD									
F5	60	0.05	0.60	0.01	5	196.93 ± 1.24	0.21 ± 0.09	25.67 ± 0.39	94.40 ± 0.34
F6	60	0.05	0.60	0.02	5	197.11 ± 2.06	0.28 ± 0.05	25.21 ± 0.26	96.42 ± 0.18
F7	60	0.05	0.60	0.05	5	201.46 ± 1.45	0.31 ± 0.18	24.98 ± 0.65	88.21 ± 0.29
Optimization of Tween-80									
F8	60	0.05	0.15	0.02	5	204.13 ± 1.17	0.35 ± 0.01	23.25 ± 0.26	70.05 ± 2.08
F9	60	0.05	0.40	0.02	5	199.24 ± 1.01	0.28 ± 0.05	24.56 ± 0.37	97.01 ± 0.18
F10	60	0.05	0.60	0.02	5	197.11 ± 2.06	0.28 ± 0.05	25.21 ± 0.26	96.42 ± 0.18
Optimization of mannitol									
F11	60	0.05	0.40	0.02	0	210.76 ± 2.12	0.31 ± 0.09	25.67 ± 0.39	91.32 ± 1.03
F12	60	0.05	0.40	0.02	5	199.24 ± 1.01	0.28 ± 0.05	24.56 ± 0.37	97.01 ± 0.18
F13	60	0.05	0.40	0.02	10	199.01 ± 2.57	0.29 ± 0.13	25.80 ± 0.12	94.40 ± 0.34

PS, particle size; *PDI,* poly disperse index; *ZP*, zeta potential; *EE*, entrapment efficiency; *FLD*, felodipine

described above after dissolved in methanol. The EE and DL could be calculated by the following equations:

$$EE\ (\%) = (W_t - W_f)/W_t \times 100\% \quad (1)$$

$$DL(\%) = (W_t - W_f)/W_0 \times 100\% \quad (2)$$

Where W_t is the amount of total drug in SLNs, W_f is the amount of free drug in SLNs, and W_0 is the amount of total SLNs.

Differential Scanning Calorimetry (DSC)

DSC studies were carried out to study the physical integrity of the drug in the SLN. The DSC thermograms of pure drug (FLD), pure lipid (glyceryl behenate), their physical mixtures, and optimized FLD-SLNs formulation were obtained by microcalorimeter (NETZSCH TG-DSC STA-449 F3, Germany). Samples were heated under nitrogen atmosphere on an aluminum pan at a rate of 10°C/min, with the temperature ranging from 30 to 400°C (34,35).

X-Ray Diffraction (XRD)

The XRD was done to monitor the changes in crystallinity characteristics of the drug loaded into SLN. The XRD patterns of pure FLD, glyceryl behenate, physical mixtures of FLD with glyceryl behenate, and optimized FLD-SLNs formulation were measured using X' D/MAX-2500/PC diffract meter (Rigaku Corporation, Tokyo, Japan) using a copper anode (Cu Ka radiation, $k = 0.15405$ nm, 40 KV, 40 mA) (35,36).

Transmission Electron Microscopy (TEM)

The morphology of FLD-SLNs was observed by transmission electron microscopy (H-7500; Hitachi Ltd., Tokyo, Japan). Apply a proper amount of water-diluted solid freeze-dried nanoparticles suspension on the copper mesh to allow the liquid to cover the entire copper mesh as much as possible and stay on the copper network for a few minutes. Then stained with saturated solution of uranyl acetate, and observed the morphology of FLD-SLNs under transmission electron microscopy after dried (37).

IN VITRO DRUG RELEASE

The dialysis membrane diffusion technique was used to study behavior of *in vitro* drug release (6,38). Two milliliters of freshly prepared FLD-SLNs (2.5 mg/mL) and free FLD suspension dispersed in 0.5% w/v CMC-Na solution as control were placed into the dialysis bags (molecular weight cut-off (MWCO) 8000–14,000) and tightly sealed, respectively. The release medium was composed of phosphate buffer with 0.4% w/v HTAB (pH 6.5) and 1% ethanol. The test bags were soaked in release medium, and the entire system was kept at 37°C and continuous magnetic stirring at the rate of 100 rpm. Samples (5 mL) were withdrawn from the release medium at predetermined time intervals and replaced by the same volume of fresh medium with the same temperature. The concentration of FLD was analyzed by UV-visible spectrophotometer at 361 nm and calculated with the standard curve ($A = 0.0164C + 0.016$, $R = 0.9997$). The following equation was used to determine similarity factor (f_2) of FLD-SLNs by the *in vitro* accumulative release (39).

$$f_2 = 50 \times \log\left\{\left[1 + (1/n)^2\right] - 0.5 \times 100\right\} \quad (3)$$

PHARMACOKINETICS EVALUATIONS

Animal Experiment

Six male beagle dogs weighing 9–10 kg were randomly divided into two groups, each comprising three beagle dogs. Food was withdrawn 12 h prior to the *in vivo* study but allowed water *ad libitum*. Group 1 and group 2 were treated with FLD-SLNs capsules and the raw FLD capsules at a dose of 30 mg/kg equivalent to FLD, respectively. Blood samples (2 mL) were collected at the following intervals: 5, 10, 15, 30, 45, 60, 120, 240, 480, 720, and 1440 min after dosing. A randomized two-stage cross-over trial was adopted in the experiment with a two-week washout period. The plasma samples were separated immediately by centrifuging the blood at 5000 rpm for 3 min and stored at − 20°C for further analysis.

Sample Extraction

FLD was extracted from the plasma samples by a liquid-liquid extraction method (24). Briefly, 200 μL of saturated sodium carbonate (Na_2CO_3) solution and 2 mL of ethyl acetate were added to 1 mL of beagle dog plasma samples successively, which was vortexed for 30 s and 3 min, respectively. After centrifugation at 10000 rpm for 5 min, the supernatant was collected. The process was repeated for twice, while all of the supernatants were mixed together and evaporated to dryness at 40°C under nitrogen. The residual was reconstituted with 200 μL of acetonitrile and centrifuged at 10000 rpm for 10 min, after which 20 μL of the clear supernatant was injected into the HPLC system for analysis.

Chromatographic Condition

HPLC was used to measure the plasma FLD concentration. Separation was achieved on a reverse phase C18 column (Phenomenex C18, 4.6 × 150 mm, 5 μm particle size, USA) with protect column (Phenomenex C18, 4.0 × 3.0 mm, 5 μm particle size, USA) at 30°C using a mobile phase of acetonitrile-deionized water (65:35 v/v) at the flow rate of 1.0 mL/min. The sample was analyzed at the wavelength of 254 nm.

STATISTICAL ANALYSIS

All pharmacokinetic parameters, including the area under the plasma drug concentration-time curve ($AUC_{0-\infty}$), the time to reach the maximum plasma drug concentration

(T_{max}), the maximum plasma drug concentration (C_{max}), the elimination half-life ($t_{1/2}$), and the mean residence time (MRT) were calculated using DAS 2.0 software.

Student's *t* test was used to evaluate the differences between the pharmacokinetic data of FLD-SLNs and free FLD suspension. All data was represented as mean ± standard error of the mean and the level of significance was at $P < 0.05$.

RESULTS AND DISCUSSION

Preparation and Optimization

Various factors that may affect the quality of FLD-SLNs were investigated (Table I), which consisted of the amount of lipid, surfactants, cryoprotectant, and drug. The ZP of all formulations was almost unaffected (maintained at 24.17–26.24 mV). This probably due to composition of the formulations was not changed. The encapsulation of a hydrophobic drug is significantly affected by the lipid which is an important component of SLNs (40). Different amounts of lipid (glyceryl behenate) were used to prepare the FLD-SLNs. EE was increased first and then decreased with increments in the glyceryl behenate concentration (ranged from 80.29 ± 0.54 to 96.42 ± 0.18). SLNs formulation prepared with 0.05 g glyceryl behenate resulted in a higher drug entrapment. Surfactants play a crucial role in stabilization of SLNs. The formulation F8–F10 showed the particle size was decreased and the EE was increased from 70.05 ± 2.08 to 97.01 ± 0.18 with the increase of Tween-80. When the dosage of Tween-80 was 0.4 g, the EE was the largest. This may be due to the solubilizing capability of Tween-80 (25,41,42). In addition, the nanoparticles system is instability and the particle size would increase, when the SLNs are stored in a water-dispersed system. The freeze-dry method can improve the stability of SLNs and the cryoprotectant can maintain the stability of the lipid membrane structure (43). The mannitol was selected as the cryoprotectant and its proper dosage for FLD-SLNs was also investigated. The particle size and PDI of the formulation without mannitol (F11) were 210.76 ± 2.12 and 0.31 ± 0.09, respectively, which were larger than that of the formulations with mannitol (F12, F13). The 5% (m/v) of mannitol was found to be optimum for entrapment efficiency, reached to 97.01 ± 0.18%. Finally, in order to obtain higher drug loading, while ensuring optimal encapsulation efficiency, 0.02 g of FLD was chosen for the further study.

Based on the results of single factor experiment, it was found that the EE of FLD-SLNs was a parameter greatly affected by excipients. And since the oral bioavailability of insoluble drug was closely related to the encapsulated amount (44), EE was selected as the evaluation index of orthogonal experiment. The result of orthogonal design experiments was shown in Table II. The values of ranged analysis represented the influence order of the factors. Therefore, the influence order of the four was D (Tween-80) > A (glyceryl behenate) > B (mannitol) > C (FLD). K1, K2, and K3 represented the sum value of each level. Analytical results of three factors were A: 1 > 2 > 3; B:1 > 2 > 3; C:3 > 2 > 1; D:3 > 2 > 1, so the best prescription was A1B1C3D3. The analysis of variance showed that factor A, B, and D had a significant effect on the EE (the values of *p* were 0.021, 0.036 and 0.003, respectively), while C had no significant effect on the result ($p = 0.465$), which was consistent with the results of intuitive analysis. Therefore, the optimal formulation was composed of FLD (0.04 g), mannitol 5% (m/v), glyceryl behenate (0.03 g), Tween-80 (0.4 g), citric acid (0.05 g), poloxamer 188 2% (m/v), and 10 mL of 0.75% (w/v) sodium bicarbonate. Three batches of samples were prepared using the optimal formulation for the following characteristic assessment.

Table II. The design and results of orthogonal table ($n = 3$)

NO.	A (g)	B (g/100 mL)	C (g)	D (g)	EE (%)
1	0.03	5	0.02	0.2	69.11 ± 2.52
2	0.03	7.5	0.03	0.3	89.84 ± 1.02
3	0.03	10	0.04	0.4	95.92 ± 0.87
4	0.04	5	0.03	0.4	94.36 ± 0.79
5	0.04	7.5	0.04	0.2	44.99 ± 3.07
6	0.04	10	0.02	0.3	61.08 ± 2.26
7	0.05	5	0.04	0.3	80.76 ± 1.82
8	0.05	7.5	0.02	0.4	75.46 ± 0.75
9	0.05	10	0.03	0.2	25.52 ± 4.61
K1	254.87	244.23	205.65	139.62	
K2	200.43	210.29	209.72	231.68	
K3	181.74	182.52	221.67	265.74	
R	73.13	61.71	16.02	126.12	

EE, entrapment efficiency

Confirmatory Test

The DL, EE, PS, ZP, and PDI of three batches of FLD-SLNs samples prepared by the optimized formulation were measured and the results were shown in Table III. The results showed that the PS of the three batches were 198.30 ± 2.82 nm, 198.06 ± 0.50 nm, and 198.10 ± 1.01 nm, respectively. The PDIs of the three batches were 0.28 ± 0.01, 0.25 ± 0.01, and 0.25 ± 0.05, respectively, indicating a homogeneous size distribution. The ZPs were − 25.90 ± 0.39 mV, − 24.9 ± 0.06 mV, and − 25.8 ± 0.13 mV, respectively. And a higher ZP (> 15 mV) means a greater electrostatic repulsion between the particles of FLD-SLNs, which helps to prevent aggregation and keep stable (23,35,45). The average of the EE and DL of the three batches samples were 95.65 ± 0.70% and 2.33 ± 0.10%, respectively. Characteristics of the three batches were not significantly different ($p > 0.05$), suggesting the excellent reproducibility of the optimized formulation.

Characterization of FLD-SLNs

Differential Scanning Calorimetry (DSC)

DSC was used to determine the compatibility status of the drug and lipid used in the FLD-SLNs formulation. DSC thermograms of pure FLD, glyceryl behenate, physical mixture of FLD with glyceryl behenate, and lyophilized FLD-SLNs formulation were presented in Fig. 2. The pure FLD displayed a sharp endothermic peak at 148.77°C, representing the melting point of the crystalline form. The result is in agreement with a previous report (15). The thermal curves of glyceryl behenate showed endothermic

Table III. Characterization of three batches of FLD-SLNs ($n = 3$)

Parameters	Batches			
	NO.1	NO.2	NO.3	Mean
PS (nm)	198.30 ± 2.82	198.06 ± 0.5	198.10 ± 1.01	198.15 ± 1.82
PDI	0.28 ± 0.01	0.25 ± 0.01	0.25 ± 0.05	0.26 ± 0.02
ZP (-mV)	25.90 ± 0.39	24.90 ± 0.06	25.80 ± 0.13	25.53 ± 0.60
EE (%)	95.34 ± 0.69	95.32 ± 0.36	96.28 ± 0.65	95.65 ± 0.70
DL (%)	2.35 ± 0.11	2.25 ± 0.08	2.38 ± 0.07	2.33 ± 0.10

PS, particle size; *PDI*, poly dispersity index; *ZP*, zeta potential; *EE*, entrapment efficiency; *DL*, drug loading; *FLD*, felodipine; *FLD-SLNs*, felodipine-loaded solid lipid nanoparticles

peak at 69.66°C and was consistent with earlier reports (46,47). The physical mixture showed FLD peak at 145.77°C and endothermic peaks of lipid at 66.33°C, which were slightly shifted to a lower temperature. These deviations could be due to the mixing effect of drug and lipid, which resulted in loss of purity of each component (35). There was no endothermic peak of FLD in the SLNs formulation indicated the conversion into amorphous state form native crystalline state of drug.

X-Ray Diffraction (XRD)

The XRD patterns of pure FLD, glyceryl behenate, their physical mixtures, and FLD-SLNs formulation were shown in Fig. 3. The figures indicated the changes in the drug crystal structure. XRD pattern of FLD have given sharp peak at 2θ angles of 10.35, 14.46, 18.86, 23.48, 29.55, 38.79, and 44.14 degrees, indicating the crystalline nature of drug. These characteristic peaks of FLD existed in physical mixtures. However, the absence of FLD peaks in SLNs formulation was observed, indicating that FLD did not existed in the crystalline state. Furthermore, the SLNs samples showed a decrease in the intensity of lipid peaks. The date of XRD was in good agreement with the DSC studies. The change in crystallinity of drug and lipid would influence the release of FLD from the SLNs, and is expected to improve the solubility of drug in water resulting in a better bioavailability (35,48).

Transmission Electron Microscopy (TEM)

A transmission electron microscopy was used to observe the physical properties of the optimized FLD-SLNs. The result revealed that the morphology of FLD-SLNs was spherical (Fig. 4a).

In vitro Drug Release

According to the previous research, a phosphate buffer with 0.4% w/v hexadecyl trimethyl ammonium bromide (HTAB) was used to simulate intestinal fluid (49). Due to the low solubility of FLD in the buffer, a small amount of ethanol was added to meet the sink condition (49). Figure 4b showed the *in vitro* release profiles of FLD-SLNs and free FLD. During the first 12 h, the release rate of FLD from the SLNs was slightly slower than that of free FLD due to the inhibition of glyceryl behenate matrix. As summarized by Kumar et al., the sustained release behavior of SLNs suggests the drug-enriched core model. In the model, the drug-loaded core is encapsulated by a lipid shell which is almost drug-free. This causes an increase in diffusional distance that hinders the drug release rate and produces sustained release effect (16,45). The amount of FLD released from the suspension was only 87.52% after 24 h, while the FLD in SLNs was almost completely released. This may be due to SLNs had a smaller particle size and a larger surface area, increased

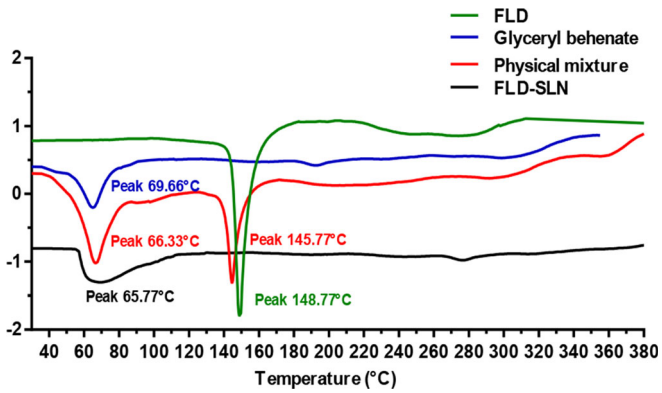

Fig. 2. The differential scanning calorimetry (DSC) thermograms of pure FLD, glyceryl behenate, physical mixture of FLD with glyceryl behenate, and FLD-SLNs

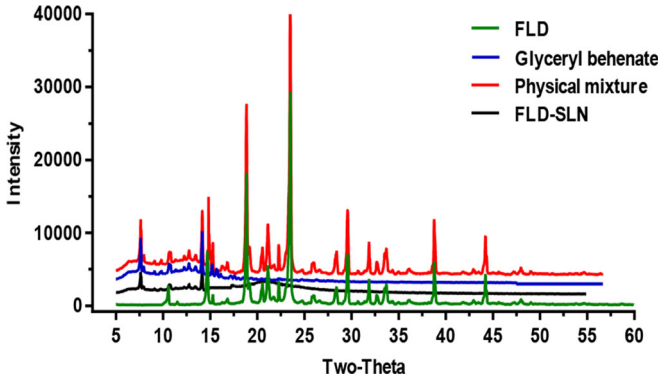

Fig. 3. X-ray diffraction (XRD) pattern of FLD, glyceryl behenate, physical mixture of FLD with glyceryl behenate, and FLD-SLNs

solubility of FLD (50). In particular, the surfactants were presented in the SLN dispersion, which could diffuse to the receiver compartment and influence the permeability of aqueous boundary layer and the barrier membrane to increase the drug release (51). And the similarity factors (*f2*) of the *in vitro* release of three batches samples were 90 (1 *vs.* 2), 95 (2 *vs.* 3), and 92 (1 *vs.*3), respectively. The values of *f2* were higher than 50, indicating that the three batches of samples had similar drug release behavior (32).

Pharmacokinetics

The relative oral bioavailability of FLD-SLNs was measured with raw FLD as a control. In this study, the HPLC analysis method was developed and validated to determine FLD in beagle dog plasma (Fig. 5a, b, c). No significant interfering peaks at or near the retention time of FLD was observed, indicating good selectivity of the chromatographic conditions. Good linearity between the peak area and the FLD concentration was found over the range of 4.0–200.0 ng/mL ($r \geq 0.999$). The intra- and inter-day assay of precision for plasma samples ranged from 3.59 to 13.67% and the accuracy was 87.06 to 98.37%. The extraction recoveries ranged from 85.67 to 103.71%. Therefore, this HPLC analysis method of biosamples could meet the requirement of determination of FLD in beagle dog plasma.

The plasma drug concentration-time profiles and the main pharmacokinetic parameters are presented in Fig.5d and Table IV, respectively. A significant difference between the pharmacokinetic behavior of FLD-SLNs and free FLD was observed (Fig. 5d). The plasma drug concentration curve of SLN showed significant improvement in drug absorption than the reference. The peak concentration (C_{max}) of FLD from SLNs was 319.42 μg/L, about 9.15 times that of free FLD (34.9 μg/L) ($P < 0.05$). The $AUC_{(0\text{-}t)}$ value of FLD in beagle dogs treated with FLD-SLNs was 68,779.475 μg/L*min, was increased more than 3.17-fold than that of free FLD (21,711.2 μg/L*min) ($P < 0.05$) (15).

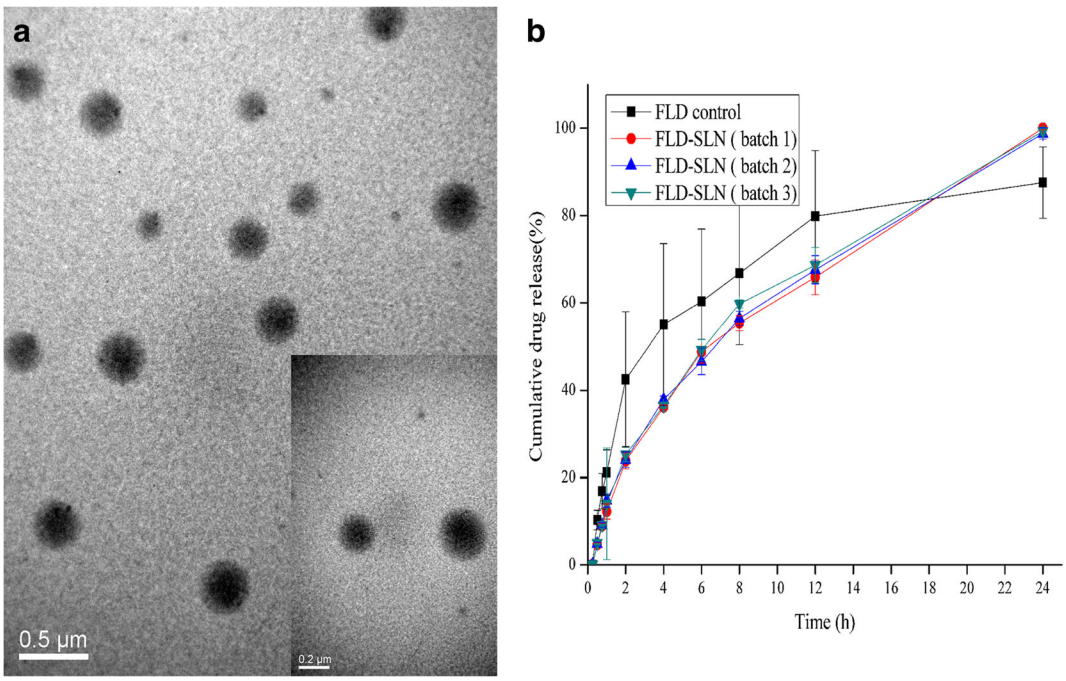

Fig. 4. **a** Transmission electron microscopy of FLD-SLNs in ultrapure water, **b** *in vitro* release curves of FLD-SLNs and raw FLD suspension ($n = 3$)

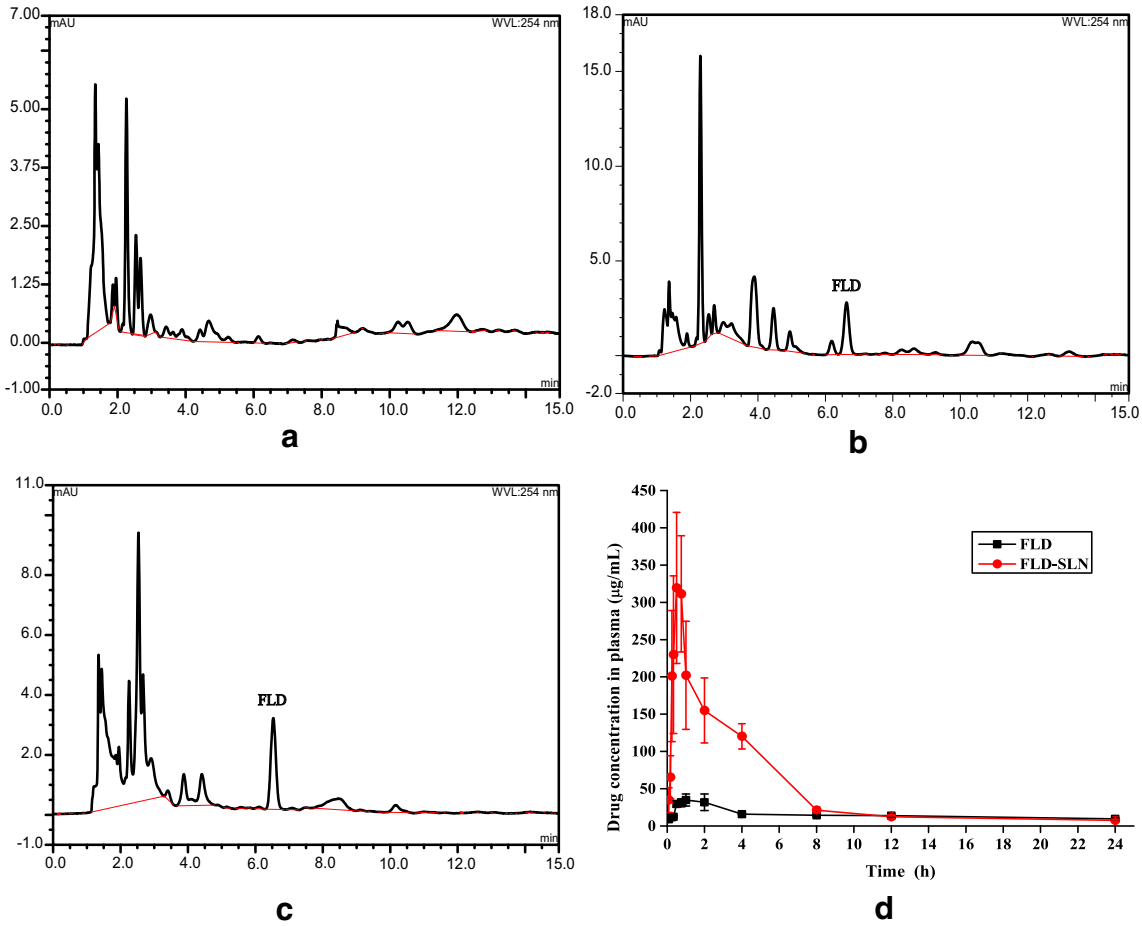

Fig. 5. Representative HPLC chromatograms of FLD in beagle plasma determined by HPLC method. **a** Blank beagle dog plasma, **b** blank beagle dog plasma spiked with FLD, **c** plasma beagle dog sample collected after oral administration of FLD-SLNs, and **d** plasma concentration-time curves of FLD after oral administration of FLD-SLNs and FLD suspension to beagle dogs, in a dose corresponding to 30 mg ($n = 6$)

The enhancement in oral bioavailability may be related to the composition and performance of FLD-SLNs (52). On the one hand, the SLNs can form a hydrophobic core to encase FLD, which increases the solubility and stability of FLD. And the small size and large surface area of the SLNs probably could increase the contact area of the drug with the intestine, thereby increasing the rate and amount of intestinal absorption of the drug (53,54). On the other hand, it may be due to the SLNs was absorbed into the systemic circulation through the lymphatic pathway, thereby reducing liver first-pass metabolism (55,56).

Table IV. Main pharmacokinetic parameters of beagle dogs

Parameters	Units	FLD-SN	FLD
$AUC_{(0\text{-}t)}$	μg/L*min	68,779.475	21,711.2
C_{max}	μg/L	319.42	34.9

AUC, area under the plasma drug concentration-time curve; *Cmax,* maximum plasma drug concentration; *FLD,* felodipine; *FLD-SLNs*, felodipine-loaded solid lipid nanoparticles

CONCLUSION

The modified effervescent dispersion technique is a reliable and manufacturable method for preparing SLNs. Compared with the previous method, the new one not only retains the advantages of foaming, which allows the nanoparticles to be distributed quickly and evenly in water, and reduces the preparation steps, making the process easier and more operable. In the present study, a novel FLD-SLN formulation was successfully obtained by effervescent dispersion technique and improved the oral bioavailability of FLD. In conclusion, SLNs was an effective carrier to improve the oral bioavailability of FLD and exhibited great potential for future clinical application.

ACKNOWLEDGMENTS

This study was financially supported by the Science and Technology Fund for Distinguished Young Scholars of Sichuan Province (No.2017JQ0013) and Basic Research (No.2016JY0192), the Joint Fund of Luzhou City and Southwest Medical University (No.2017LZXNYD-T02), the scientific research Foundation of the Education Department of Sichuan Province (No.17ZA0439, 18ZB0646), and the scientific research Foundation of Southwest Medical University (No.2016-63).

COMPLIANCE WITH ETHICAL STANDARDS

Conflict of Interest The authors declare that they have no conflicts of interest in this work.

Ethical Approval The animal studies were approved by the Committee on the Ethics of Animal Experiments of the Southwest Medical University (No 2015DW040).

REFERENCES

1. Lu Y, Lv Y, Li T. Hybrid drug nanocrystals. Adv Drug Deliv Rev. 2019;143:115–33.
2. Wu W, Lu Y, Qi J. Editorial: persistent endeavors for the enhancement of dissolution and oral bioavailability. Acta Pharm Sin B. 2019;9(1):2–3.
3. Huang W, Wu X, Qi J, Zhu Q, Wu W, Lu Y, et al. Ionic liquids: green and tailor-made solvents in drug delivery. Drug Discov Today. 2019;S1359–6446(19):30378–2.
4. Ren X, Qi J, Wu W, Yin Z, Li T, Lu Y. Development of carrier-free nanocrystals of poorly water-soluble drugs by exploring metastable zone of nucleation. Acta Pharm Sin B. 2019;9(1):118–27.
5. Liu D, Wan B, Qi J, Dong X, Zhao W, Wu W, et al. Permeation into but not across the cornea: bioimaging of intact nanoemulsions and nanosuspensions using aggregation-caused quenching probes. Chinese Chem Lett. 2018;29(12):1834–183 8.
6. Sahu BP, Das MK. Nanosuspension for enhancement of oral bioavailability of felodipine. Appl Nanosci. 2014;4(2):189–97.
7. Patel PK. Solid dispersion as a formulation strategy: a mini review. J Chem and Lifesci. 2017;6(6):2039–45.
8. Parashar D, Rajendran V, Shukla R. Lipid-based nanocarriers for delivery of small interfering RNA for therapeutic use. Eur J Pharm Sci. 2019;142:105159.
9. Liu C, Liu D, Bai F. In vitro and in vivo studies of lipid-based nanocarriers for oral N3-o-toluyl-fluorouracil delivery. Drug Deliv. 2010;17:352–63.
10. Rehman A, Tong Q, Jafari SM, Assadpour E, Shehzad Q, Aadil RM, et al. Carotenoid-loaded nanocarriers: a comprehensive review. Adv Colloid Interf Sci. 2019;7:102048.
11. Porter CJ, Trevaskis NL, Charman WN. Lipids and lipid-based formulations: optimizing the oral delivery of lipophilic drugs. Nat Rev Drug Discov. 2007;6(3):231–48.
12. Qi J, Zhuang J, Lu Y, Dong X, Zhao W, Wu W. In vivo fate of lipid-based nanoparticles. Drug Discov Today. 2017;22:166–72.
13. Hu X, Fan W, Yu Z, Lu Y, Qi J, Zhang J, et al. Evidence does not support absorption of intact solid lipid nanoparticles via oral delivery. Nanoscale. 2016;8(13):7024–35.
14. Hu X, Zhang J, Yu Z, Xie Y, He H, Qi J, et al. Environment-responsive aza-BODIPY dyes quenching in water as potentialprobes to visualize the in vivo fate of lipid-based nanocarriers. Nanomedicine. 2015;11(8):1939–48.
15. Gondrala UK, Dudhipala N, Kishan V. Preparation, characterization and in vivo evaluation of felodipine solid-lipid nanoparticles for improved oral bioavailability. Int J Pharm Sci Nanotech. 2015;8(4):2995–3002.
16. Kumar VV, Chandrasekar D, Ramakrishna S, Kishan V, Rao YM, Diwan PV. Development and evaluation of nitrendipine loaded solid lipid nanoparticles: influence of wax and glyceride lipids on plasma pharmacokinetics. Int J Pharm. 2007;335:167–75.
17. Chalikwar SS, Belgamwar VS, Talele VR, Surana SJ, Patil MU. Formulation and evaluation of Nimodipine-loaded solid lipid nanoparticles delivered via lymphatic transport system. Colloids Surf B: Biointerfaces. 2012;97:109–16.
18. Ekambaram P, Abdul HSA. Formulation and evaluation of solid lipid nanoparticles of ramipril. J Young Pharm. 2011;3(3):216–20.
19. Parmar B, Mandal S, Petkar KC, Patel LD, Sawant KK. Valsartan loaded solid lipid nanoparticles: development, characterization and in vitro and ex vivo evaluation. Int J Pharm Sci. 2011;1(3):1483–90.
20. Naseri N, Valizadeh H. Solid lipid nanoparticles and nanostructured lipid carriers: structure, preparation and application. Adv Pharm Bull. 2015;5:305–13.
21. Mehnert W, Mäder K. Solid lipid nanoparticles production, characterization and applications. Adv Drug Deliv Rev. 2001;47(2–3):165–96.
22. Domb AJ. Lipospheres for controlled delivery of substances. United States Patent. 1993, USS 188837.
23. Zhao L, Ye Y, Li J, Wei Y. Preparation and the in-vivo evaluation of paclitaxel liposomes for lung targeting delivery in dogs. J Pharm Pharmacol. 2011;63(1):80–6.
24. Wei Y, Xue Z, Ye Y, Huang Y, Zhao L. Paclitaxel targeting to lungs by way of liposomes prepared by the effervescent dispersion technique. Arch Pharm Res. 2014;37(6):728–37.
25. Zhao L, Wei Y, Li W, Liu Y, Wang Y, Zhong X, et al. Solid dispersion and effervescent techniques used to prepare docetaxel liposomes for lung-targeted delivery system: in vitro and in vivo evaluation. J Drug Target. 2011;19(3):171–8.
26. Yuan JY, Pi C, Huang SQ, Liang J, Feng T, Zhan CL, et al. Development and evaluation of felodipine sustained-release tablets. Lat Am J Pharm. 2018;37(1):73–9.
27. Little WC, Cheng CP, Elvelin L, Nordlander M. Vascular selective calcium entry blockers in the treatment of cardiovascular disorders: focus on felodipine. Cardiovasc Drugs Ther. 1995;9(5):657–63.
28. Li D, Xu S, Wang Y, Li X, Pan J. Pharmacokinetics and drug-drug interaction between enalapril, enalaprilat and felodipine extended release (ER) in healthy subjects. Oncotarget. 2017;8(41):70752–60.
29. Sahu BP, Das MK. Preparation and in vitro/in vivo evaluation of felodipine nanosuspension. Eur J Drug Metab Pharmacokinet. 2014;39(3):183–93.
30. Navadiya K, Tiwari S. Pharmacology, efficacy and safety of felodipine with a focus on hypertension and angina pectoris. Curr Drug Saf. 2015;10(3):194–201.
31. Sandeep SM, Sridhar V, Puneeth Y, Babu PR, Babu KN. Enhanced oral bioavailability of felodipine by naringenin in Wistar rats and inhibition of P-glycoprotein in everted rat gut sacs in vitro. Drug Dev Ind Pharm. 2014;40(10):1371–7.
32. Singh M, Kanoujia J, Parashar P, Arya M, Tripathi CB, Sinha VR, et al. Assessment of improved buccal permeation and bioavailability of felodipine microemulsion-based cross-linked polycarbophil gel. Drug Deliv Transl Res. 2018;8(3):1–11.
33. Rigon RB, Fachinetti N, Severino P, Santana MH, Chorilli M. Skin delivery and in vitro biological evaluation of trans-resveratrol-loaded solid lipid nanoparticles for skin disorder therapies. Molecules. 2016;21(1):E116.
34. Yan HM, Zhang ZH, Jiang YR, Ding DM, Sun E, Jia XB. An attempt to stabilize tanshinone IIA solid dispersion by the use of ternary systems with nano-CaCO3 and poloxamer 188. Pharmacogn Mag. 2014;10(Suppl 2):S311–7.
35. Dudhipala N, Veerabrahma K. Improved anti-hyperlipidemic activity of rosuvastatin calcium via lipid nanoparticles: pharmacokinetic and pharmacodynamic evaluation. Eur J Pharm Biopharm. 2017;10:47–57.
36. Bhalla S, Nagpal M. Comparison of various generations of superporous hydrogels based on chitosan-acrylamide and in vitro drug release. ISRN Pharm. 2013;2013(2):624841.
37. Xiao X, Zhu WW, Yuan H, Li WW, Li Q, Yu HQ. Biosynthesis of FeS nanoparticles from contaminant degradation in one single system. Biochem Eng J. 2016;105:214–9.
38. Wan F, You J, Sun Y, Zhang XG, Cui FD, Du YZ, et al. Studies on PEG-modified SLNs loading vinorelbine bitartrate (I): preparation and evaluation in vitro. Int J Pharm. 2008;359(1–2):104–10.
39. Ochiuz L, Popa G, Stoleriu I, Tomoiaga AM, Popa M. Microencapsulation of metoprolol tartrate into chitosan for

improved oral administration and patient compliance. Ind Eng Chem Res. 2013;52(49):17432–41.
40. Pathade AD, Kommineni N, Bulbake U. Preparation and comparison of oral bioavailability for different nano-formulations of Olaparib. AAPS PharmSciTech. 2019;20:276.
41. Alam T, Pandit J, Vohora D, Aqil M, Ali A, Sultana Y. Optimization of nanostructured lipid carriers of lamotrigine for brain delivery: in vitro characterization and in vivo efficacy in epilepsy. Expert Opin Drug Deliv. 2015;12(2):181–94.
42. Ahmad I, Pandit J, Sultana Y, Mishra AK, Hazari PP, Aqil M. Optimization by design of etoposide loaded solid lipid nanoparticles for ocular delivery: characterization, pharmacokinetic and deposition study. Mater Sci Eng C Mater Biol Appl. 2019;100:959–70.
43. Soares S, Fonte P, Costa A. Effect of freeze-drying, cryoprotectants and storage conditions on the stability of secondary structure of insulin-loaded solid lipid nanoparticles. Int J Pharm. 2013;456:370–81.
44. Ong SG, Ming LC, Lee KS, Yuen KH. Influence of the encapsulation efficiency and size of liposome on the oral bioavailability of griseofulvin-loaded liposomes. Pharmaceutics. 2016;8(3):E25.
45. Silki SVR. Enhancement of in vivo efficacy and oral bioavailability of aripiprazole with solid lipid nanoparticles. AAPS Pharm Sci Tech. 2018;9(3):1264–73.
46. Kai C, Shou LI, Kai J. Formulation optimization of indomethacin-loading solid lipid nanoparticles by box-Behnken response surface methodology. China Pharmacy. 2016;27(22):3118–20.
47. Brubach JB, Jannin V, Mahler B. Structural and thermal characterization of glyceryl behenate by X-ray diffraction coupled to differential calorimetry and infrared spectroscopy. Int J Pharm. 2007;336(2):248–56.
48. Roberta C, Otto C, Maria EC, Michele T, Carmela S, Maria RG. Sterilization and freeze-drying of drug-free and drug loaded solid lipid nanoparticles. Int J Pharm. 1997;148:47–54.
49. Pi C, Feng T, Liang J, Zhan CL, Wei YM, Zhao. Polymer blends used to develop felodipine-loaded hollow microspheres for improved oral bioavailability. Int J Biol Macromol. 2018;112:1038–47.
50. Zhao L, Wei Y, Huang Y, He B, Zhou Y, Fu J. Nanoemulsion improves the oral bioavailability of baicalin in rats: in vitro and in vivo evaluation. Int J Nanomedicine. 2013;8:3769–79.
51. Yang S, Li K. Dissolution profile study on the novel doxycycline hydrochloride sustained-release capsules. Pak J Pharm Sci. 2014;27(5 Suppl):1615–20.
52. Zhang Z, Gao F, Bu H, Xiao J, Li Y. Solid lipid nanoparticles loading candesartan cilexetil enhance oral bioavailability: in vitro characteristics and absorption mechanism in rats. Nanomedicine. 2012;8(5):740–7.
53. Trevaskis NL, Charman WN, Porter CJ. Lipid-based delivery systems and intestinal lymphatic drug transport: a mechanistic update. Adv Drug Deliv Rev. 2008;60(6):702–16.
54. Harde H, Das M, Jain S. Solid lipid nanoparticles: an oral bioavailability enhancer vehicle. Expert Opin Drug Deliv. 2011;8(11):1407–24.
55. Reddy RN, Shariff A. Solid lipid nanoparticles: an advanced drug delivery system. Int J Pharm Sci Rev Res. 2013;4:161–71.
56. Patel RR, Chaurasia S, Khan G, Chaubey P, Kumar N, Mishra B. Highly water-soluble mast cell stabiliser-encapsulated solid lipid nanoparticles with enhanced oral bioavailability. J Microencapsul. 2016;33(3):209–20.